

ULTRASONOGRAPHY- A TOOL ITS MECHANICS AND DENTAL APPLICATIONS

¹Dr. Aachut Pandav, ²Dr. Vijay Namdevrao Yannawar, ³Dr. Shivam Agrawal, ⁴Dr. Valaja Kamble and ⁵Dr. Pratik Parkarwar¹Sr. Lecturer. Dept of Conservative Dentistry & Endodontics. Dr. HSRSM Dental College and Hospital Hingoli.²Sr. Lecturer. Dr. HSRSM Dental College and Hospital Hingoli.³Sr. Lecturer. Dept of Orthodontics and Dentofacial Orthopedic. Dr.HSRSM Dental College and Hospital. Hingoli.⁴Tutor. Dept of Oral and Maxillofacial Surgery. PDU Dental College Solapur.⁵Sr. Lecturer. Dept of Oral Medicine and Radiology. PDU Dental College, Solapur.***Corresponding Author: Dr. Pratik. Parkarwar**

Sr. Lecturer. Dept of Oral Medicine and Radiology. PDU Dental College, Solapur.

Article Received on 05/10/2020

Article Revised on 25/10/2020

Article Accepted on 15/11/2020

ABSTRACT

Ultrasonography is one of the the popular frequent imaging modality used in dental with medical sciences. The use of ultrasonography after discovery was used as a therapeutic aid, but now a days, it has become one of the the majority common imaging modality subsequently to conventional radiology. Definitive diagnosis of any lesion or pathology is obtained with help of diagnostic aids like imaging, lab investigation, histo pathological examination etc. Many imaging techniques were available in addition to conventional x rays. Among advanced imaging ultrasonography is a widely available, non ionizing, relatively inexpensive and easily reproducible imaging modality which uses an oscillating sound pressure wave with a frequency greater than the upper limit of the human hearing range. Nowadays therapeutic ultrasound is most widely used and accepted as an adjuvant treatment modality for patients with pain, musculoskeletal disorders, soft tissue inflammation and swelling. The biological/physiological interactions at tissue level were sufficiently evolved in the last century which leads to further advancement in therapeutic ultrasound when a sound wave propagates through the medium. This paper reviews on both diagnostic and therapeutic ultrasound in dentistry.

KEYWORDS: Specialized, therapeutics, ultrasonography, pathology, musculoskeletal, sound waves.**INTRODUCTION**

Ultrasound imaging is easy to use for the detection of noninvasive and soft tissue-related diseases. Ultrasonography utilizes sound waves for image production. The first major attempt at a practical application was made in search for the **sunken Titanic in the North Atlantic in 1912**. A few early attempts at applying US in medical diagnosis Successful medical application began shortly after the war in the late 1940s and early 1950s.

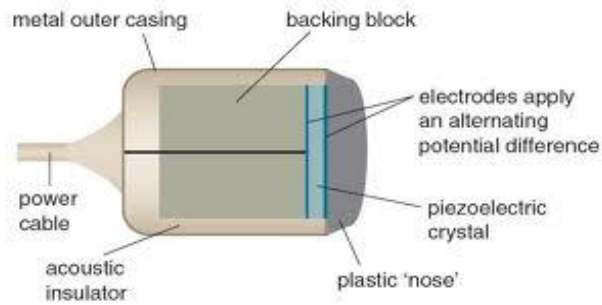
The vital ingredients are **transducer, ultrasonic beam, a cathode ray tube or television monitor**. The evolution of sonic imaging began slowly from a static one dimensional base (**A-mode or amplitude mode**), improved somewhat when a component of motion was added (**TM-mode**), made a giant leap forward with 2 dimensional imaging (**B mode or brightness mode**) and reached its current zenith with gray scale imaging.

The phenomenon perceived sound is the result of periodic changes in the pressure of air against the eardrum. The periodicity of these changes lies anywhere between **1500 and 20,000 cycles per second (hertz**

[Hz]). By definition, ultrasound has a periodicity greater than **20 kHz**. Thus it is distinguished from other mechanical waveforms simply by having a vibratory frequency greater than the audible range.

Diagnostic ultrasonography (sonography), the clinical application of ultrasound, uses vibratory frequencies in the range of **1 to 20 MHz**. Scanners used for sonography generate electrical impulses that are converted into ultra-high-frequency sound waves by a transducer.

Transducer is a device that can convert one form of energy into another-in this case, electrical energy into sonic energy. The most important component of the transducer is a thin **piezoelectric crystal** or material made up of a great number of dipoles arranged in a geometric pattern. A dipole may be thought of as a distorted molecule that appears to have a positive charge on one end and a negative charge on the other



Currently, the most widely used piezoelectric material is **lead zirconate titanate (PZT)**. The electrical impulse generated by the scanner causes the dipoles in the crystal to realign themselves with the electrical field and thus suddenly change the crystal's thickness. This abrupt change begins a series of vibrations that produce the sound waves that are transmitted into the tissues being examined. As the ultrasonic beam passes through or interacts with tissues of different **acoustic impedance**, it is attenuated by a combination of **absorption, reflection, refraction, and diffusion**.

Sonic waves that are reflected back (echoed) toward the transducer cause a change in the thickness of the piezoelectric crystal, which in turn produces an electrical signal that is amplified, processed, and ultimately displayed as an image on a monitor. In this system the transducer serves as both a transmitter and a receiver.

Current techniques permit echoes to be processed at a sufficiently rapid rate to allow perception of motion; this is referred to as **real time imaging**. In contrast to x-ray imaging, in which the image is produced by transmitted radiation, the reflected portion of the beam produces the image in sonography. The fraction of the beam that is reflected back to the transducer depends on the acoustic impedance of the tissue, which is a product of its density (and thus the velocity of sound through it) and the **beam's angle of incidence**.

Because of its acoustic impedance, a tissue has a characteristic internal echo pattern. Consequently, not only can changes in echo patterns delineate different tissues, but they also can be correlated with pathologic changes in a tissue. Interpretation of sonograms, therefore, relies on knowledge of both the physical properties of ultrasound and the anatomy of the tissues being scanned.

Ultrasound waves are both transmitted and received by the probe, and the image is constructed by complex computerized analysis of the reflected and scattered waves that return from the interrogated tissues. Superior resolution is obtained using high frequency sound waves at the expense of depth penetration. Typically, in the **head and neck region linear 8–12MHz** probes are used whereas in the **abdomen** a lower frequency probe (**usually 3.5–5 MHz**) is essential to achieve adequate depth. Ultrasound waves are scattered in air so a contact

gel that bridges the interface between the skin and the probe is essential to optimise transmission. Gas contained within tissues such as in an abscess, will also cause ultrasonic scatter, which results in a **“white out”**.

The cortex of bone and other calcified structures such as salivary duct calculi transmit sound poorly with almost total reflection and result in acoustic shadowing. Highly reflective tissues with poor transmission appear **echogenic (white)**, whereas structures with poor reflectivity but excellent transmission such as blood that is moving in the internal jugular vein will be **hypoechoic (black)** on an image.

The high reflectivity of both metallic needles and foreign bodies is advantageous in facilitating ultrasound-guided biopsy examinations and localisation procedures, respectively. As an adjunct to structural imaging, **color** (directional) and **power Doppler** (non-directional but more sensitive) are often used to assess blood flow and the vascularity of tissue. These techniques add value in detecting abnormal peripheral or **chaotic flow** patterns in malignant lymph nodes, in assessing the patency of normal vessels, and in the investigation of **vascular and lymphatic malformations**.

The following features were considered in describing the ultrasonographic images of swelling in the head and neck in accordance with Shimizu *et al.*^[52]

Shape: oval, lobular, round, polygonal, irregular;

Boundary: very clear, relatively clear, partially unclear, ill defined;

Echo intensity: anechoic, isoechoic, hypoechoic, hyperechoic, mixed;

Ultrasound architecture of lesion: homogeneous, heterogeneous;

Presence of necrosis: eccentric, central;

Presence of calcification: macrocalcification, microcalcification; posterior echoes: enhanced, unchanged, attenuated; and Ultrasound characteristic of tissues: cystic, solid, mixed.

A mass is **hypoechoic** if it has a intensity lower than that of the adjacent tissue.

Hyperechoic is used for masses of higher intensity and **isoechoic** is used for masses with intensity similar to the adjacent tissue. The appearance of hypoechoic masses is darker whereas the hyperechoic masses appear rather bright, and the isoechoic ones have a similar appearance. A calcified mass appears hyperechoic and a clear fluid or blood appears anechoic.

The internal echoes may be either **homogeneous or heterogeneous**.

'**Homogeneous**', refers to an even echo pattern or reflections that are relative and uniform in composition. If the mass is uniformly hypoechoic or hyperechoic, then it is described as a homogeneous mass.

'**Heterogeneous**', refers to an uneven echo pattern or reflections of varying echodensities. If a mass lesion contains hyperechoic and hypoechoic areas, it would be described as a heterogeneous mass.

'**Acoustic enhancement**', is the increased echogenicity (echo brightness) of tissues that lie behind a structure that causes little or no attenuation of the ultrasound waves, such as a fluid-filled cyst. The opposite of **acoustic enhancement is acoustic shadowing**.

Clinical applications of ultrasonography in maxillofacial region

For differentiating between **periapical cysts & granulomas**. **Elegra Siemens** apparatus with a regular size, linear, high definition, multifrequency US probe at a frequency of 709 MHz is used. US probe gloved and positioned on the buccal sulcus of the maxillary bone corresponding to the apical areas of teeth.

So, the cystic lesion appeared as **hypoechoic**, well contoured cavity, surrounded by reinforced bone walls, filled with fluids & with no evidence of internal vasculature on color Doppler US. While the granuloma appeared as **corpused (hyperechoic/ echogenic)** or could show both corpused and hypoechoic areas, exhibiting a rich vascular supply.

Cystic structures are **anechoic** because liquids are homogeneous, and there are **no acoustic interfaces** to generate internal echoes. There is little or no attenuation of the sound as it passes through a cystic structure, which creates the appearance of enhanced transmission of the sound at the distal aspect of a cystic mass.

The **dentigerous cysts** exhibited anechoic to focal hyperechogenicity with heterogeneously distributed internal echoes. The focal hyperechogenicity in the anechoic area of the dentigerous cysts was the tooth portion which helps to differentiate between radicular cyst and dentigerous cyst. This was one of the important findings observed in their study of bony cysts.

Their study revealed that on ultrasonography **bony cysts** appeared anechoic with homogeneously distributed internal echo pattern and unchanged posterior wall echo. The soft tissue cyst had similar ultrasonographic findings of bony cysts with posterior wall echo enhancement.

The **abscesses** too exhibited similar ultrasonographic findings of the soft tissue cyst, but with an irregular walled boundary echo. Soft tissue abscesses have variable

sonographic appearances; however, they are typically anechoic or hypoechoic, well-defined, with posterior acoustic enhancement and possible anechoic fluid motion during transducer compression, and hypervascularity.

Abscesses present with heterogeneous hypoechogenicity, ill-defined margins, lobulated contour, solid and cystic composition, moderate size, moderate Resistive Index, with hyperechogenicity in the subcutaneous layer, and hypervascularity, especially on the margin of the lesion. In addition to US findings, clinical symptoms such as infectious signs are also important.

Fascial space spread of odontogenic infections- Acc to a study by **Maaly Bassiony et al** US is an effective method in detecting & staging spread of odontogenic infections to the superficial spaces. However, it might be difficult to detect deep fascial involvements. Edematous changes appear isoechoic but with increased fluid contents. **Cellulitis** appear as hyperechoic than normal due to inflammation. **Preabscess** were mixed & abscess appeared as anechoic.

Salivary glands

Ultrasound readily shows whether a lesion is within or is external to a salivary gland. **Normal parotid and submandibular glands** have a homogeneous echotexture on ultrasound. The concept of the superficial parotid lobe is defined on ultrasound as being superficial to the well-visualised retromandibular vein; this latter structure acts as a surrogate marker for the more superficial intraparotid facial nerve.

In the axial plane, the normal **Stenson's duct** may be seen as paired and parallel echogenic lines 3mm apart overlying the masseter muscle. In the floor of the mouth Wharton's duct travels with the neurovascular bundle and is usually visualised only when it is pathologically dilated. **Lymph nodes** in the submandibular space are always located external to the salivary gland while in contrast intraparotid lymph nodes are often encountered.

Salivary stones-Intraglandular calculi lying within glandular soft tissue are more easily identified than **extraglandular ductal stones**, which are surrounded by air within the mucosal folds of the oral cavity. Ultrasound is helpful in detecting sialoliths and in the diagnosis of conditions involving the salivary.^[53]

Frank dilatation of the duct or **sialectasis** easily seen, and ultrasound can often show the complications of calculi such as the formation of **abscesses and sialoceles**. It cannot totally exclude calculi and, if there is a strong clinical suggestion of distal ductal obstruction and the ultrasound study is negative, occlusal dental radiography and sialography may still be required.

Sialadenitis of the salivary gland exhibited hypoechoic internal echo pattern with focal hypoechogenicity in cases of sialolithiasis.

Inflammation-Inflammatory conditions of the major salivary glands should initially be investigated with ultrasound. **Acute inflammation** causes swelling and hypoechogenicity, with loss of the normal glandular homogeneous bright echotexture. It reliably detects formation of an abscess and may show hyperreflective **microbubbles of gas** in **suppurative sialadenitis** with adjacent reactive nodes. In the case of abscess formation in acute suppurative sialadenitis,

Ultrasound-guided percutaneous drainage can be combined with antibiotics to avoid surgical intervention. Two chronic conditions result in a distinctive “leopard skin” or “currant cake” appearance, namely **juvenile chronic sialadenitis** and **Sjögren syndrome**.

In **Sjögren disease** the changes are classically bilateral. They affect the parotid and submandibular glands and are associated with dry eyes and a dry mouth. Typically, in **juvenile chronic sialadenitis** there is unilateral change. The classic clinical and ultrasound findings of Sjögren disease obviate the need for sialography. It is associated with **extra-nodal lymphoma**, which may present as a hypoechoic mass within an affected major salivary gland.

Benign salivary gland tumor

Benign salivary gland tumors exhibited lobular shape with smooth walled to well-defined boundary echo but malignant salivary gland tumor exhibited irregularly walled to poorly defined boundary echo and shape could not be classified.

Pleomorphic adenoma-On ultrasound it appears as a well-defined, hypoechoic, homogeneous, solid mass with a lobulated border and low-level internal vascularity, which may display posterior acoustic enhancement. Smaller adjacent daughter lesions are often identified, but cervical lymphadenopathy is not usually seen.

Warthin tumour (adenolymphoma)-The tumors are usually well circumscribed on ultrasound, and are typically heterogeneous with cystic and solid areas. They may appear pseudocystic and non-compressible with through-transmission of sound (posterior acoustic enhancement).

Malignant tumors of the salivary glands

Primary malignant tumors of the salivary glands such as mucoepidermoid, adenoid cystic, and acinar cell carcinomas, occur disproportionately more often in the sublingual and submandibular glands than in the parotid glands. Features suggestive of malignancy include poorly defined margins with inherent heterogeneous

echotexture, disorganized color flow, and the presence of associated abnormal lymph nodes.

Assessment of cervical lymphadenopathy

The criteria for the use of ultrasound in the assessment of lymph nodes have been extensively described. **Normal nodes** have a well-defined fusiform, kidney bean shape with an intermediate or low reflectivity, homogeneous cortex, and a highly reflective central hilus. The length of the node is not considered as important as the dimension of the short axis, which should not normally exceed 10 mm.

A width to length ratio greater than 0.5 implies a rounded abnormal node, and the more rounded a node, the more likely it is to contain metastatic disease. Notably, in the **submandibular and submental** regions normal nodes tend to be more rounded, so shape alone should not be used as an isolated predictor of malignancy.

Intranodal vessels are visible with color imaging, and in benign nodes flow is typically central or hilar in distribution. **Abnormal nodes** tend to be hypoechoic or “black” with cortical thickening and a tendency to lose the central echogenic hilus. Short axis measurements increase with loss of the normal ovoid configuration, and nodal vascularity may increase with a chaotic pattern.

In particular, peripheral or subcapsular vessels are a strong sign of malignancy. Difficulty may arise with **lymphoma-infiltrated lymph nodes** that characteristically appear rounded, but often retain a central echogenic hilus, and appear homogeneous and hypoechoic (pseudocystic). Color flow imaging often shows an exaggerated benign blood flow pattern (termed **plethoric hilar vascularity**).

The **lymph node swellings** exhibited hypoechoic internal echo pattern. **Dystrophic calcification** of the lymph node appeared as multiple focal hyperechogenicity within the hypoechoic internal echo pattern.^[28] Doppler US evaluates the vascular pattern of nodes and helps to identify the malignant nodes. Normal lymph nodes have extensive vascularity originating in the hilus and branching radially towards the periphery.

US can be used to assess lymph nodes in patients with oral cancers. Many studies have reported the usefulness of US for the diagnosis of lymph node metastases.^[61,62,63] In these reports, ultrasound scanning had a diagnostic accuracy rate of about 90% in cervical lymph node staging.^[64,65, 66]

Benign odontogenic tumors

Benign odontogenic tumors had hyperechoic to anechoic internal echo pattern with heterogeneously distributed internal echoes and benign nonodontogenic tumor had hypoechoic internal echo pattern with homogeneously distributed internal echoes.

Lipoma-Most lipomas occur in the superficial soft tissues and are generally slightly **hyperechoic** relative to the surrounding fat lobule or muscle; however, they sometimes appear **isoechoic** or **hypoechoic**. Most lipomas present specific patterns of “**parallel echogenic lines**” or focal homogeneous hyperechogenicity. On Color Doppler US (CDUS), most lipomas present as **avascular**; weak vascularity is observed within the tumor in a small number of patients.

Hemangioma-The typical ultrasonographic patterns are heterogeneous echogenicity, ill-defined margins, solid and cystic in composition, and hypervascularity; however, good compressibility, echogenic rim, and the presence of **phleboliths** have very high positive predictive value for hemangioma

Giant cell tumor-The typical patterns in giant cell tumor are heterogeneous hypoechogenicity, ovoid or lobulated contour, solid composition, moderate size and located along the tendon. Although the US pattern of most GCT of tendon sheath includes a well-defined margin and moderate resistive index (RI), this pattern is not statistically significant. The ultrasonographic features are, however, nonspecific and indistinguishable from other types of **synovitis**. **Giant cell tumors** also tend to have a heterogeneous echotexture with areas of necrosis. Fluid levels may be seen.

Malignant swellings

Malignant swellings exhibited a shape which could not be classified with irregularly walled or irregularly walled to poorly defined boundary echo pattern. A significant association was observed between clinical, ultrasonographic and histopathological diagnoses. Like other imaging techniques it is not possible to suggest the true nature of the disease by ultrasonography for which one should rely on histopathology.^[28] Acc to **Satoru Shintani et al** US is superior to CT & MRI in assessment of primary lesion of oral carcinoma.^[31]

Interventional Radiology Using Fine-Needle Aspiration by Ultrasonography-**Nao Wakasugi-Sato et al** injected **OK-432 (picibanil)**, a biological response modifier used for **sclerotherapy**, into masses as nonsurgical treatment for **ranulas** in the oral floor. **Roh and Kim** reported total or nearly total shrinkage in six of nine cases of ranulas. In a follow up after the last sclerotherapy, recurrence of the ranula was observed in only one patient. No significant complications were observed; four patients reported fever and mild local pain lasting for 2–4 days after treatment. Others reported that seven (33%) of 21 patients with plunging ranulas showed total shrinkage and resolution.

This technique using US seems to be effective for **OK-432** administration to masses as a nonsurgical treatment for ranulas in the oral floor. So, US images can be applied for both confirmation of the appropriate removal

of cystic fluid from the ranula & for confirmation of **OK-432** administration into the ranula.

Tumor thickness in oral squamous cell carcinoma of the tongue

Tumor thickness is highly related to the occurrence of cervical metastasis. Accurate preoperative assessment is indispensable to improve therapeutic effects. Particularly in cases of tongue cancer, US imaging is often used to accurately estimate tumor size or thickness and to define adequate resection margins with tumor extension and deep infiltration.

Exostosis -The features of exostosis in most patients are heterogeneous hyperechogenicity with well-defined margins, lobulated contour, solid content, with calcification, hypoechoic cartilage cap, moderate size, and relative hypovascularity or mild vascularity on CDUS.

Some patients present with a bony protrusion from the cortex and away from the joint, with a thin hypoechoic cap covering the protruding bone. The hypoechoic cartilage cap in exostosis is commonly less than 2 cm in diameter

Lymphangioma- The characteristic finding of lymphangioma is multiloculated cystic with septation. In most patients, the features are heterogeneous hypoechogenicity with ill-defined margins, lobulated contour, solid and cystic inner contents, large size, and avascularity or mild vascularity on CDUS.

In some patients, a **tortuous tubular structure** is apparent within the lesion, and some have bleeding within the cystic component. The echogenic component possibly correlates to the cluster of abnormal lymphatic channels that are too small to reflect the sound beam. Large lesions have ill-defined boundaries with cystic components that dissect normal tissue planes.

Traumatic neuroma-The typical ultrasonography findings are heterogeneous hypoechogenicity, ill-defined margins, ovoid contour, and solid inner content, small or moderate size, and avascular or hypovascular on CDUS.

Fibromatosis-Griffith et al report that most palmar fibromatosis presents as hypoechoic and is well-defined, with posterior enhancement and hypervascularity. It also presents as heterogeneous hypoechogenicity with infiltrated margins, lobulated contour if well-defined in margin, solid content, moderate to large size, and mild to moderate vascularity with moderate RI on CDUS. If the tumor is close to the bone, irregularity may occur over the bony cortex.

Myositis ossificans- It commonly involves the limbs, with lamellar bone forms at the periphery of the lesion that proceed toward its center. The centrifugal pattern of

calcification and ossification presents as a “zoning” phenomenon on **computed tomography**.

The ultrasound findings of myositis ossificans are heterogeneous hyperechogenicity, ill-defined margins, lobulated shape, solid content, large size, and grade 2 on CDUS, with moderate RI and prominent segmental calcification.

Hematoma-Typical patterns of hematoma are heterogeneously hypoechogenicity, well- or ill-defined margins, and avascularity on CDUS.

Pseudoaneurysm-The characteristic appearance of pseudoaneurysm is the extraluminal pattern of blood flow, which shows variable echogenicity, interval complexity, and to-and-fro flow pattern on CDUS.

Chronic inflammation or granulomatous lesions-The typical patterns in chronic inflammation or granulomatous lesions are heterogeneous hypoechogenicity, ill-defined margins, lobulated morphology, solid composition, moderate size, and moderate RI.

Foreign body retention-Foreign body retention usually appears as heterogeneous echogenicity, with well- or ill-defined margins, ovoid contour, solid content, small size, and mild to moderate hypervascularity on CDUS, with echogenic foreign bodies present within the lesion.

Varix-Varix is a focal dilatation of the venous system that commonly presents as an echo-free or heterogeneously hypoechogenicity, with well-defined margins, ovoid contour, cystic inner content, moderate size, moderate vascularity or thrombus on CDUS, and turbulent flow pattern. The sacular cystic structure should connect to the vessel during tracing.

Primary bone tumors-The inability of diagnostic US to penetrate adult cortical bone limits its usefulness in the assessment of primary bone pathologies and it has been suggested that US has no role in the evaluation of bone tumors. However, once an aggressive benign or malignant tumor has penetrated the cortex to produce a subperiosteal or extraosseous mass, this part of the tumor becomes accessible to US evaluation, since it is only covered by muscle, subcutaneous fat and skin. Similarly, tumors arising from the surface of the bone can be imaged with US.

(A) **Periosteum**- US can identify the unmineralized raised periosteum as a well-defined thin hyperechoic line. Once the periosteum has mineralized, it appears as a smooth continuation of the cortex at the extraosseous tumour margin, equivalent to the **Codman's triangle** identified on plain radiographs.

(B) **Cortex** -The normal cortex of a long bone appears as a relatively thick hyperechoic line with a well-

defined smooth outer surface and posterior acoustic shadowing. US can demonstrate a grossly intact cortex in the case of lesions arising from a juxtacortical location and also cortical erosion from more aggressive surface sarcomas.

Cortical destruction from medullary tumors, particularly osteosarcoma, appears as discontinuity or marked irregularity of the smooth hyperechoic line of the normal cortex. Pathological fracture is identified as a break and step in the hyperechoic line of the cortex with or without an associated extraosseous tumour mass.

(C) **Neurovascular bundle** - The neurovascular bundle may be either encased or displaced by tumors with large extraosseous components most commonly arising in the metaphyses of long bones. The presence or absence of flow within vessels can be clearly determined using color Doppler.

(D) **Tumor matrix**-Turnout mineralization appears as irregular hyperechoic areas within the extraosseous mass which may or may not be associated with acoustic shadowing, depending upon the degree of matrix ossification.

Osteogenic sarcoma (OGS)

Most OGSs with soft tissue involvement present with heterogeneous hyperechogenicity, infiltrated margins, scalloped contour, solid composition, large size, moderate hypervascularity on CDUS, and moderate RI. Surrounding bony destruction, bony fragments, and sunburst periosteal reaction is observed in most patients. Recurrence of OGS may appear as a well-defined ovoid hypoechoic nodule that differs from the original OGS.

Lytic osteosarcoma typically has a heterogeneous echotexture, commonly with well defined anechoic areas corresponding to tumour necrosis. **Ewing's sarcoma** and peripheral neuroectodermal tumor (PNET), can also have a variable appearance. Tumors with a relatively small extraosseous component appear homogeneously hypoechoic. However, once they become large and undergo a degree of necrosis, the matrix becomes heterogeneous and may not be distinguishable from osteosarcoma.

Chondrosarcoma appears as a multilobulated mass with the lobules being relatively homogeneously hypoechoic. US appearances of matrix mineralization will mirror those seen on the plain radiograph, being either punctate hyperechoic areas or more extensive curvilinear hyperechoic areas with distal acoustic shadowing

Fluid-fluid levels and septation may be identified in **Aneurysmal bone cysts** (ABC) when these lie in a subperiosteal location.

Color Doppler may also be useful in assessing the vascularity of a lesion. The majority of osteosarcomas and GCTs are hypervascular and regions of either **pulsed-type or continuous-type** flow may be identified within the same tumour. **Round-cell tumour** and **chondrosarcoma** are relatively hypovascular.^[32]

Metastasis

The origin of most metastases is from carcinoma, rarely from sarcoma. Most are moderate or large in size, with heterogeneous hypoechogenicity, infiltrated margins, scalloped contour, solid composition, moderate hypervascularity on CDUS, and moderate RI. Tumors located close to the bony cortex commonly result in surrounding bony destruction.

Lymphoma

Peripheral soft tissue lymphoma can present as mass, nodal, nodular, myositis, and cellulitis types. The ultrasonographic pattern of peripheral soft tissue lymphoma depends on the type. The typical pattern for the mass, nodal, and myositis types of peripheral lymphoma is relatively homogeneous hypoechogenicity, infiltrated margins, scalloped contour, solid composition, large size, and marked hypervascularity on CDUS.

In the **nodular type** the typical presentation is multiple small hypoechoic nodules with hypervascularity. In the cellulitis type, the typical presentation is echogenic subcutaneous fat lobules, ill-defined margins, and hypervascularity. They also found that the mass and nodal types are the most common types of peripheral soft tissue lymphoma.

In ultrasonography, there is the facility of on-screen nodal measurement.^[69]

Small round-cell tumor

Small round-cell tumor contains conventional neuroblastoma, rhabdomyosarcoma, lymphoma, and Ewing sarcoma. Ultrasonography is nonspecific and may reveal mixed echogenicity with or without cystic components. In our experience, it could appear with heterogeneous hypoechogenicity, infiltrated margins, scalloped contour, solid content, large size, moderate vascularity on CDUS, and low RI.

Rhabdomyosarcoma

Rhabdomyosarcoma is the most common soft tissue malignancy in children, but is rare in the extremities. The role of ultrasound is to provide information regarding tumor size and internal characteristics, and in guided biopsy. CDUS can determine vascularity but does not aid in differential diagnosis. The ultrasonographic pattern is heterogeneous hypoechogenicity, infiltrated margins, lobulated contour, solid content, moderate size, moderate vascularity on CDUS, and moderate RI.

Fibrosarcoma - Ultrasonography of fibrosarcoma typically reveals heterogeneous hypoechogenicity, ill-defined margins, ovoid contour, solid content, large size, mild vascularity on CDUS, and moderate RI.

Ultrasonography of the temporomandibular joint

For the evaluation of

1. TMJ disk position,
2. joint effusion,
3. Osteoarthritis

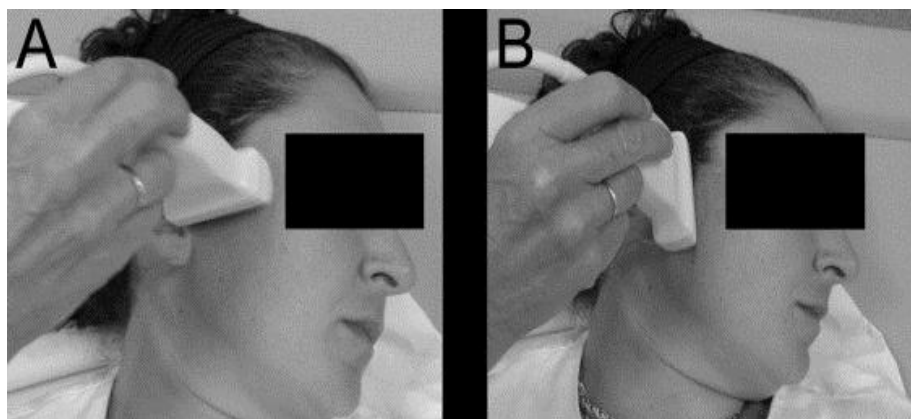


Fig. 37-Transverse scan longitudinal scans.

The imaging protocol includes transverse and longitudinal scans so the antero-superior joint compartment can be examined in coronal, axial and oblique views a satisfactory view is obtained, **static and dynamic** evaluations are usually performed at different mouth opening positions (Fig-37).

Cortical bone tissues, such as the head of the condyle and the glenoid fossa, are generally hyperechoic

appearing white on US images, while bone marrow is usually hypoechoic and appears black. **Connective** (joint capsule and retrodiscal area) and **muscular tissues** (lateral pterygoid and masseter muscles) are isoechoic and appear heterogeneously grey in US images.

Empty spaces and water (superior and inferior joint spaces) are hypoechoic (black), even though they are

virtual cavities that are usually not detectable, unless effusion is present. The articular disk consists of dense fibrocartilaginous tissue, and usually appears as a thin area of hyperechogenicity surrounded by a hypoechoic halo, even though its depiction with US is controversial.

Ultrasonographically:- Diagnostic accuracy of US to detect disk displacement ranged from 62% to 100%. One of the major shortcomings of US is represented by the deviation and abnormal reflection of ultrasounds when they intercept hard tissues, therefore it appears impossible to recognize the disk when it is placed between two hard structures and far from the ultrasound source.

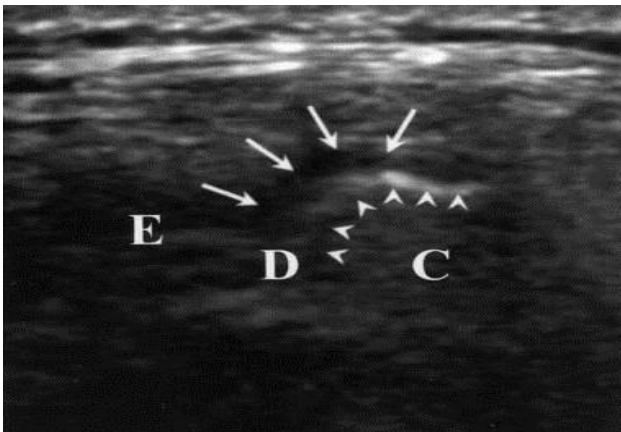


Fig. 38.

Articular disk is usually hypo- to isoechoic, and that echogenicity increases with disk degeneration. Artifacts in disk echogenicity may be present if the orientation of the sonographic beam is not exactly the same as the disk surface. Temporomandibular joint with disk displacement showing anterosuperior TMJ compartment and disk (arrows) superior to condyle (arrowheads). E = articular eminence, D = disk, C = condyle.

Joint effusion

Direct visualization of a hypoechoic area within the articular space or by an indirect measurement of capsular distension, taken as the distance between condylar latero-superior surface and the articular capsule (a hyperechoic line running parallel to the surface of the mandibular condyle) with the subject in the closed-mouth position.

Receiver operating characteristic (ROC) curve analysis suggested that the critical area is that around the 2 mm TMJ capsular width value (lower values had high sensitivity; higher values had high specificity).

Osteoarthritis

Joint space narrowing, abnormalities of condylar surface, erosions is commonly based on the detection of an interruption or absence of the echogenicity of the cortical lining. Owing to the deflection of sound waves by bone structures, the medial aspect of the condyle can hardly be depicted, and **osteophyte formation** and condylar

erosion are more easily seen in the **anterior or lateral aspect** of the condyle. Condylar morphology is best seen on longitudinal scans, but transverse investigation may help to increase the examiner's confidence that the condyle has osteoarthritis. Ultrasound that clinical diagnosis had a sensitivity and accuracy of 85.7% and ultrasonographic diagnosis had a sensitivity and accuracy of 98.5%.

Advantages of ultrasonography

- Noninvasive nature
- No radiation exposure so safe in pregnancy
- Easy reproducibility
- Possibility of real time imaging
- Ability to detect non calcified pathological entities such as sialoliths.
- Widely available
- Relatively rapid diagnostic US is estimated to be less expensive^[71] US is more patient friendly as claustrophobia, which is not encountered with US imaging.^[72]
- Diagnostic US also examine large areas with extended field of view (FOV) imaging, however the clinician can interact with the patient who can then direct the examination toward the symptomatic area.^[73]

Limitations of ultrasonography

- Bone and air are absolute barrier to an ultrasound beam. Some regions are difficult or impossible to examine because of technical limits.
- Significance of an examination is extremely dependent on experience of examiners.

Disadvantages of ultrasonography

- Images can be difficult to interpret for inexperienced operator because image resolution is often poor.
- Technique is operator dependent
- Real-time imaging means that the radiologist must be present during the investigation.

Future developments

High Intensity Focused Ultrasonography
Magnetic Resonance Imaging-Guided
Focused Ultrasound Surgery
Ultrasound Guided Ablation
Sonoporation
Low-Intensity Pulsed Ultrasonography
Ultrasound-Guided Drainage of Deep
Neck Space
Extracorporeal Lithotripsy
Elastography,

BIBLIOGRAPHY

1. Tomography at the US National Library of Medicine Medical Subject Headings (MeSH)
2. white and pharoh pg, 247.

3. Fuji N and Yamashiro M. Computed tomography for the diagnosis of facial fractures, *J oral surg*, 1981; 39: 735.
4. Kassel EE , Noyek AM and Cooper PW. CT in facial trauma. *J Otolaryngol*, 1983; 12: 2-5.
5. Abrahams JJ, Caceres C. Mandibular erosion from silastic implants: evaluation with a dental CT software program. *AJNR Am J Neuroradiol*, 1998; 19: 519-522.
6. Roithmann R, Kassel EE, Kirsch JC, Wortzman G, Abrahams JJ, Noyek AM. New radiographic techniques for detection of mandibular invasion by cancer. *Oper Tech Otolaryngol Head Neck Surg*, 1993; 2: 149-154.
7. Yanagisawa K, Friedman C, Abrahams JJ. DentaScan imaging of the mandible and maxilla. *Head Neck*, 1993; 14: 979-990.
8. Abrahams JJ, Olivario P. Odonotogenic cysts: improved imaging with a dental CT software program. *AJNR Am J Neuroradiol*, 1993; 14: 367-374.
9. Abrahams JJ, Berger S. Inflammatory disease of the jaw: appearance on reformatted CT images. *AJR Am J Roentgenol*, 1998; 170: 1085-1091.
10. Abrahams JJ, Glassberg RM. Dental disease: a frequently unrecognized cause of maxillary sinus abnormalities?. *AJR Am J Roentgenol*, 1995; 166: 1219-1223.
11. Abrahams JJ, Berger SB. Oral-maxillary sinus fistula oroantral fistula: clinical presentation and evaluation with multiplanar CT. *AJR Am J Roentgenol*, 1995; 165: 1273-1276.
12. Abrahams JJ, Levine B. Expanded applications of DentaScan: multiplanar CT of the mandible and maxilla. *Int J Periodontics Restorative Dent*, 1990; 10: 464-467.
13. Abrahams JJ. Anatomy of the jaw revisited with a dental CT software program: pictorial essay. *AJNR Am J Neuroradiol*, 1993; 14: 979-990.
14. Lain S, Osaka F, Asanami S and Tomita O. adenocytic carcinoma in computed tomography. *Oral Surg*, 1980; 49: 552-555.
15. Ames JR , Johnson RP and Stevens EA. Computerized tomography in oral and Maxillofacial surgery. *J Oral surg.*, 1980; 38: 145-149.
16. Ames JR . Computerized tomography in oral and Maxillofacial surgery. *J Oral surg.*, 1980; 38: 145-149.
17. Cho PS, Johnson RH, Griffin TW. Cone-beam CT for radiotherapy applications. *Phys Med Biol*, 1995; 40: 1863-83.
18. Spector L. Computer-Aided Dental Implant Planning. *Dental Clinics of North America*, 2008; 52: 761-75.
19. Razavi T, Palmer RM, Davies J et al. Accuracy of measuring the cortical bone thickness adjacent to dental implants using cone beam computed tomography. *Clinical Oral Implants Research*, 2010; 21: 718-25.
20. Lewis EL, Dolwick MF, Abramowicz S, Reeder SL. Contemporary Imaging of the Temporomandibular Joint. *Dental Clinics of North America*, 2008; 52: 875-90.
21. Farman AG, Scarfe WC. The Basics of Maxillofacial Cone Beam Computed Tomography. *Seminars in Orthodontics*, 2009; 15: 2-13.
22. Patel S, Dawood A, Ford TP, Whaites E. The potential applications of cone beam computed tomography in the management of endodontic problems. *International Endodontic Journal*, 2007; 40: 818-30.
23. Spector L. Computer-Aided Dental Implant Planning. *Dental Clinics of North America*, 2008; 52: 761-75.
24. Spector L. Computer-Aided Dental Implant Planning. *Dental Clinics of North America*, 2008; 52: 761-75.
25. Thomas SL. Application of Cone-beam CT in the Office Setting. *Dental Clinics of North America*, 2008; 52: 753-9.
26. *Jiomr*, 2010; 22(1): 34-38.
27. Grant DG. Tomosynthesis: a three-dimensional radiographic imaging technique. *IEEE Trans Biomed Eng*, 1972; 19: 20 - 28.
28. Groenhius RA, Webber RL, Ruttimann UE. Computerized tomosynthesis of dental tissues. *Oral Surg Oral Med Oral Pathol*, 1983; 56: 206 - 214.
29. Webber RL, Horton RA, Tyndall DA, Ludlow JB. Tuned- aperture computed tomography (TACT1). Theory and application for three-dimensional dento-alveolar imaging. *Dentomaxillofac Radiol*, 1997; 26: 53 - 62.
30. Nair MK, Nair UP Digital and advanced imaging in endodontics: a review. *Journal of Endodontics*, 2007; 33: 1-6.
31. Webber RL, Messura JK An in vivo comparison of digital information obtained from tuned-aperture computed tomography and conventional dental radiographic imaging modalities. *Oral Surgery, Oral Medicine, Oral Pathology, Oral Radiology and Endodontology*, 1999; 88: 239-47.
32. De Coene B, Hajnal JV, Gatehouse P, Longmore DB, White SJ, Oatridge A, Pennock JM, Young IR, Bydder GM. "MR of the brain using fluid-attenuated inversion recovery (FLAIR) pulse sequences". *Am J Neuroradiol*, 1992; 13 (6): 1555-64.
33. Moseley ME, Cohen Y, Mintorovitch J, Chileuitt L, Shimizu H, Kucharczyk J, Wendland MF, Weinstein PR. "Early detection of regional cerebral ischemia in cats: Comparison of diffusion- and T₂-weighted MRI and spectroscopy". *Magn Reson Med*, 1990; 14(2): 330-46
34. Ridgway JP, Smith MA. "A technique for velocity imaging using magnetic resonance imaging". *Br J Radiol*, 1986; 59(702): 603-7
35. Takashima S, Noguchi Y, Okumura T, Aruga H, Kobayashi T. Dynamic MR imaging in the head and neck. *Radiology*, 1993; 189:813-21.

36. Asaumi J, Shigehara H, Konouchi H, et al. Assessment of carcinoma in the sublingual region based on magnetic resonance imaging. *Oncol Rep*, 2002; 9: 1283-7
37. Takashima S, Noguchi Y, Okumura T, Aruga H, Kobayashi T. Dynamic MR imaging in the head and neck. *Radiology*, 1993; 189: 813-21.
38. Asaumi J, Shigehara H, Konouchi H, et al. Assessment of carcinoma in the sublingual region based on magnetic resonance imaging. *Oncol Rep*, 2002; 9: 1283-7.
39. Fischbein NJ, Noworolski SM, Henry RG, Kaplan MJ, Dillon WP, Nelson SJ. Assessment of metastatic cervical adenopathy using dynamic contrast-enhanced MR imaging. *Am J Neuroradiol*, 2003; 24: 301-11.
40. Noworolski SM, Fischbein NJ, Kaplan MJ, et al. Challenges in dynamic contrast-enhanced MRI imaging of cervical lymph nodes to detect metastatic disease. *J Magn Reson Imaging*, 2003; 17: 455- 62.
41. Fischbein NJ, Noworolski SM, Henry RG, Kaplan MJ, Dillon WP, Nelson SJ. Assessment of metastatic cervical adenopathy using dynamic contrast-enhanced MR imaging. *Am J Neuroradiol*, 2003; 24: 301-11.
42. Noworolski SM, Fischbein NJ, Kaplan MJ, et al. Challenges in dynamic contrast-enhanced MRI imaging of cervical lymph nodes to detect metastatic disease. *J Magn Reson Imaging*, 2003; 17: 455- 62.
43. Asaumi J, Yanagi Y, Hisatomi M, Matsuzaki H, Konouchi H, Kishi K. The value of dynamic contrast-enhanced MRI in diagnosis of malignant lymphoma of the head and neck. *Eur J Radiol*, 2003; 48: 183-7.
44. Kaplan PA, Tu HK, Williams SM, Lydiatt DD. The normal temporomandibular joint: MR and arthrographic correlation. *Radiology*, 1987; 165: 177-178.
45. Drace JE, Enzmann DR. Defining the normal temporomandibular joint: closed-, partially open-, and open-mouth MR imaging of asymptomatic subjects. *Radiology*, 1990; 177: 67-71.
46. Westesson PL, Eriksson L, Kurita K. Reliability of a negative clinical temporomandibular joint examination: prevalence of disk displacement in asymptomatic temporomandibular joints. *Oral Surg Oral Med Oral Pathol*, 1989; 68: 551-554.
47. Tallents RH, Katzberg RW, Murphy W, Proskin H. Magnetic resonance imaging findings in asymptomatic volunteers and symptomatic patients with temporomandibular disorders. *J ProsthetDent*, 1996; 75: 529-533.
48. Katzberg RW, Westesson PL, Tallents RH, Drake CM. Anatomic disorders of the temporomandibular joint disc in asymptomatic subjects. *J Oral Maxillofac Surg*, 1996; 54: 147-153.
48. Algra PR, Bloem JL, Tissing H, et al. Detection of vertebral metastases: comparison between MR imaging and bone scintigraphy. *Radiographics*, 1991; 11: 219-32.
49. Avrahami E, Tadmor R, Dally O, Hadar H. Early MR demonstration of spinal metastases in patients with normal radiographs and CT and radionuclide bone scans. *J Comput Assist Tomogr*, 1989; 13: 598-602.